

Ram Accelerator Ballistic Range Concept for Softly Accelerating Hypersonic Free-Flying Models

K. Wieland Naumann*

French-German Research Institute, Saint Louis F-68301, France
and

Adam P. Bruckner†

University of Washington, Seattle, Washington 98195

Technical limitations and requirements on the state of the test gas suggest accelerating models rather than accelerating the test gas for hypervelocity testing. This holds particularly for measuring methods that necessitate longer measurement times, such as force or heating measurements, or investigations of propulsion, ablation, or re-entry in nonterrestrial atmospheres. Conveniently, recent developments in instrumentation, on-board data transmission and recording, and acceleration techniques extend the capability of free-flight experiments. In addition to general considerations, this article gives an example of the outline of a suitable test facility based on the ram accelerator hypervelocity launcher concept and its adaptation to different measuring tasks.

Nomenclature

A	= area, m ²
a	= acceleration, m/s ²
C_D	= drag coefficient
c	= speed of sound, m/s
D	= diameter, m
E	= energy, J
f	= internal degrees of freedom
L	= length, m
M	= Mach number
\mathcal{M}	= mole mass, kg/kmole
m	= mass, kg
P	= power, W
p	= pressure, Pa
R	= radius, m
T	= temperature, K
t	= time, s
U	= velocity, m/s
V	= volume, m ³
ρ	= density, kg/m ³
σ	= tensile stress, MPa

Subscripts

Bo	= body
cs	= cross section
e	= end value
eff	= effective value
ex	= exterior
F	= fin
in	= interior
Me	= measurement
Mo	= model
max	= maximum value
n	= normal direction
Proj	= projectile
Prop	= propellant

p	= permitted load
S	= sabot
T	= tube
TC	= test chamber
TF	= test flow
tot	= total value
0	= stagnation value
1	= filling state in ram tube

Superscript

-	= mean value
---	--------------

Introduction

THE term “hypervelocity aerodynamics” describes hypersonic flow in cases where the Mach number is not the only relevant parameter. For investigations of boundary-layer flow or mixing and combustion, the parameters velocity, density, gas composition, and characteristic length are important as well. An increase in the number of relevant parameters means less tolerance in scaling, and as a consequence, a requirement for more powerful testing facilities.

The power P of a wind tunnel (this term also comprises shock tunnels, Ludwig tubes, etc.) depends on the flow velocity U , flow density ρ , and test chamber cross section area A , as follows:

$$P_{TF} = 0.5 \times \rho_{TF} \times A_{TC} \times U_{TF}^3 \quad (1)$$

For example, the power of a testing facility with test chamber cross section $A_{TC} = 0.4 \times 0.4$ m, $U = 5000$ m/s, at atmospheric density $\rho = 1.225$ kg/m³, is $P_{TF} = 12.25$ GW, which can be supplied and controlled in such a comparatively small installation for at most a few milliseconds.

Another aspect is the condition of the test gas. Its acceleration in any type of test facility requires an energy supply

Table 1 Obtainable velocity of air in wind or shock tunnels and the corresponding minimum change of test gas state due to energy addition

Minimum change of test gas state	U_{TC} , m/s
No change	2,000
Dissociation of O ₂ ($T_{0,eff} = 7000$ K)	4,000
Upper limit for shock tunnels (with ionization)	8,000
Upper limit of wave expansion (with ionization)	15,000

Received Jan. 1, 1993; revision received March 9, 1994; accepted for publication March 9, 1994. Copyright © 1994 by K. W. Naumann and Adam P. Bruckner. Published by the American Institute of Aeronautics and Astronautics, Inc., with permission.

*Scientist, Department of Gas Dynamics, BP 34. Member AIAA.

†Professor, Aerospace and Energetics Research Program, Department of Aeronautics and Astronautics, FL-10. Associate Fellow AIAA.

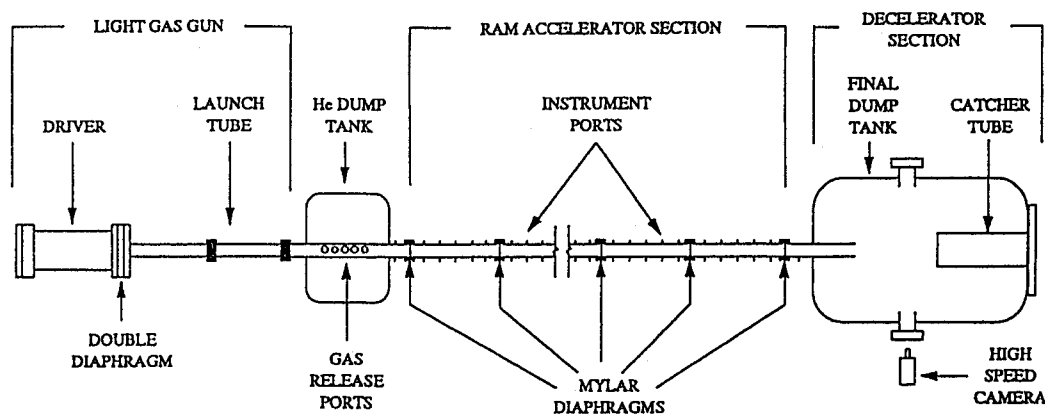


Fig. 1 Schematic of the University of Washington ram accelerator facility.

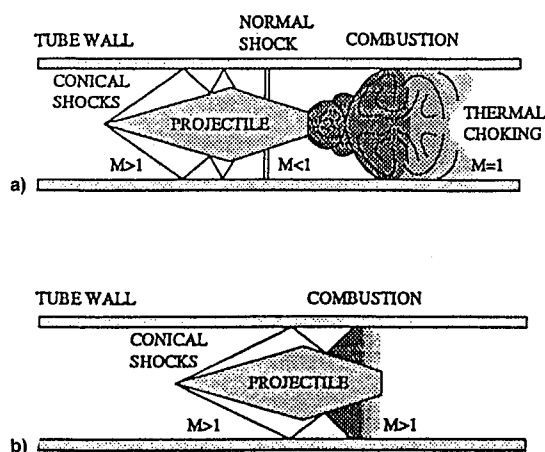


Fig. 2 Ram-acceleration of a projectile (Mach numbers in body-fixed coordinates): a) subsonic thermally choked combustion and b) supersonic combustion.

in conjunction with heating at some stage of the process. Table 1 shows the velocity of air that can be achieved and the corresponding minimum change of the test gas state, if test gas temperature equal to ambient temperature is desired in the test chamber. Note that about 2000 m/s is the maximum velocity obtainable without dissociating air during the heating process.¹ Tests on extraterrestrial atmospheres, which contain polyatomic gases such as methane, are much more sensitive to energy addition and the nondissociating velocity limit is lower.

The ability of the material of a hypervelocity tunnel to withstand the heating load caused by the necessary energy density may also be a limiting factor.² The principal detrimental effect is the contamination of the test flow with ablated material, originating from the nozzle throat.

On the other hand, for the aerodynamic parameters to be measured most easily at hypervelocity conditions, a minimum test flow slug length L_{TS} with

$$L_{TS} = t_{Me} \times U \geq 4 - 15 \times L_{Mo} \quad (2)$$

is needed to produce quasistationary aerodynamic loads.³ For the simulation of chemical reacting flows, the minimum L_{TS} and, hence, the necessary test flow duration may be longer.

In spite of these limitations, acceleration of the test gas has been to date the dominant procedure in hypervelocity aerodynamic testing with instrumented models, because it is accessible with a greater variety of measurement techniques.⁴ Other reasons are as follows:

1) Lack of a launcher capable of launching models of sufficient size and mass (several kilograms) at moderate accel-

eration levels to hypervelocities. Conventional gun launchers lose effectiveness if the launch velocity exceeds half the wave expansion velocity, $U_{max} = f \times c_0$,⁵ where f is the number of the internal degrees of freedom (DOF) of the propelling gas, and c_0 is its speed of sound. Moreover, the acceleration is not uniform, because there exists a peak acceleration and a sharp acceleration rise at the beginning of the process. This can be reduced by using a longer barrel or careful matching of the stages of a light gas gun, with some sacrifice of efficiency.⁶ Nevertheless, this peak acceleration imposes severe limits on structural design of the models and on the on-board instrumentation.

2) Lack of transducers, telemetry or memory devices, and electrical supplies, which can be packed into models, sustain heavy acceleration and produce signals of sufficient accuracy.

3) Much better access to the flowfield, if the model is at rest. Many measuring techniques cannot be applied with free-flying models; for these techniques wind-tunnel testing will invariably remain necessary.

For these reasons hypervelocity testing with accelerated models has been limited up to the present time to studies using small models that have, at most, limited on-board instrumentation.

On the other hand, the most powerful high-enthalpy facilities are free-piston driven Stalker tubes such as the T5 at the California Institute of Technology² and the HEG in Göttingen,⁷ and the free-piston-driven expansion tube at GASL.⁸ HEG and T5 are able to produce a test flow velocity greater than 5 km/s for 1–3 ms; the testing time of expansion tubes is less. Clearly these facilities represent the peak of state-of-the-art hypervelocity wind-tunnel capability.

The severe restrictions on free-flight testing due to accelerator limitations can be overcome by ram acceleration (see Ref. 9 and references therein). Moreover, progress in the state-of-the-art of transducers, storage of data, telemetry,¹⁰ and data processing opens up new prospects for hypervelocity aerodynamic testing using free-flying models. In what follows we describe a proposed test facility based on the ram accelerator principle to "softly" launch aerodynamic test models to very high velocities.

Ram Accelerator Driven Free-Flight Facility

Principle of Operation

The ram accelerator (Fig. 1) is a novel type of launcher. Its special advantages are that the projectile velocity does not depend on any typical gas velocity, and that projectile motion and gas motion are not coupled. Theoretically, this permits the attainment of projectile velocities above 10 km/s with high efficiency.⁹ The propellant is a combustible gas mixture that fills the accelerator tube. A preaccelerator, e.g., a powder- or gas-gun, provides the necessary starting velocity of about 1000 m/s. When the projectile moves inside the ram-tube, the

nose shock and subsequent reflected shock waves compress and heat the gas mixture (see Fig. 2). Combustion initiated behind or on the projectile body generates high pressure on the projectile base, exerting forward thrust.

Depending on the ratio between the projectile velocity and the detonation velocity of the undisturbed gas mixture, the combustion process is termed "subdetonative," "transdetonative," or "superdetonative."¹¹ To date, each of these modes has been demonstrated experimentally for velocities up to 2700 m/s in a 38-mm bore device of 16 m length at the University of Washington.⁹ The progress of the acceleration histories obtained indicates that higher velocities will be obtainable with longer acceleration paths.^{9,11} Recent work at ISL¹² and ARL¹³ has demonstrated operation with bore diameters of 90 and 120 mm, respectively, proving the ease of scalability of the concept.

The acceleration level to which the projectile is subjected can be easily tailored by matching the cross-sectional area load of the projectile $m_{\text{Proj}}/A_{\text{cs, Proj}}$, and the fill pressure of the accelerator tube p_1 . The acceleration can be chosen to attain any value appropriate to the structural stability of the model, the demands of the on-board instrumentation, or other criteria.

Measuring Tasks

Investigations with free-flying models can be divided into two approaches¹⁴:

1) Experiments with stably flying, unguided models, following a straight flight path. Topics to investigate are, particularly, heating, aerothermodynamics and material properties testing; boundary layers in high enthalpy flow with hot walls; scramjet propulsion; and signal transmission and optronics. In these cases the testing range can be enclosed for protection against environmental effects or for the arbitrary choice of the test atmosphere. The length of this range depends on the measuring time needed. This will be longer for experiments on aerodynamic heating and ablation than for investigations of boundary layer transition or shock related phenomena. A testing time of about 100 ms or more may be required.

2) Experiments with models producing some kind of lift or, in general, a normal force. This means investigations on hypervelocity lifting bodies; guidance, control, and stability; external combustion; and ablation and related aerothermodynamic phenomena. In these cases, the trajectories of the models are more or less curved. Usually, in this case, the model's attitude must be measured, e.g., with small laser gyros. In some cases, unpredictable trajectories may occur, e.g., as a result of erratic ablation or structural or mechanical failure of the model. The desired measuring times are on the order of 10–100 ms.

Instrumentation and Model Requirements

A key criterion is the tolerable maximum acceleration of the model. Table 2 shows that the transducers set the limiting value. This value is imposed not only by survivability, but also by the need for good resolution and accuracy. For aerodynamic force measurements in free flight (at expected loads of 10^3 – 10^4 m/s² acceleration or deceleration), a resolution of 10–100 m/s² is desirable, thus limiting the operational range of a transducer to roughly 10^5 m/s² (similar considerations hold also for pressure transducers). During the process of

model recovery higher deceleration rates may be tolerated, as long as physical survival of the instrumentation can be ensured. Electronics that tolerate about 7×10^5 m/s² are the present state of the art.¹⁰

The instrumentation necessary for task (2) above can be packed into a model of about 5-kg mass (including sabot casing) and 20-cm span. This model size represents roughly the maximum size permissible inside a test chamber of 40 cm diam. If additional installations (e.g., jets or combustibles) need to be built into the model, its size must increase accordingly, e.g., up to 50-cm span and 30 kg (assuming $m_{\text{Proj}}/A_{\text{cs, Proj}}$ is kept approximately constant). The model size for task (1) may be somewhat less. In accordance with Ref. 15 we assign 6 km/s as the peak velocity. This is well within the predicted limits of efficient operation of the ram accelerator, and aerodynamic heating loads during acceleration should not impose unsolvable problems.⁹

Concept of a Ram Accelerator Driven Free-Flight Facility

Ram Accelerator

Figure 3 shows the length of the ram accelerator tube needed as a function of terminal projectile velocity and mean acceleration. The circled point marks the preferred values, with a tube length L_T of 175 m (for acceleration from $U_{\text{Proj}} = 1000$ – 6000 m/s). For preacceleration we chose an average of 50,000 m/s², to minimize jerk load; the corresponding preaccelerator length is 10 m.

The effective pressure acting on the projectile base p_{eff} (see Table 3) ranges from 10 to $15 \times p_1$. With some allowance for friction and other losses we adopt an average $p_{\text{eff}}/p_1 \approx 8$.

Usually, the model will be packed in a sabot, which provides an optimum shape for ram acceleration and protects the model. The primary technical challenge with the sabot is to ensure aerothermal and mechanical stability of the structure, because both heat load and pressure are very high at the same time. With respect to the heat load, some degree of ablation should be tolerated in order to limit the heat flux into the interior of the structure. New ceramic materials are not only very heat resistant, but keep their full mechanical strength up to temperatures of about 1400 K, without being too brittle.¹⁵

At the side and rear parts of the body, ablation does not cause problems either with the flowfield or with combustion. At the front part of the model ablation can be tolerated to

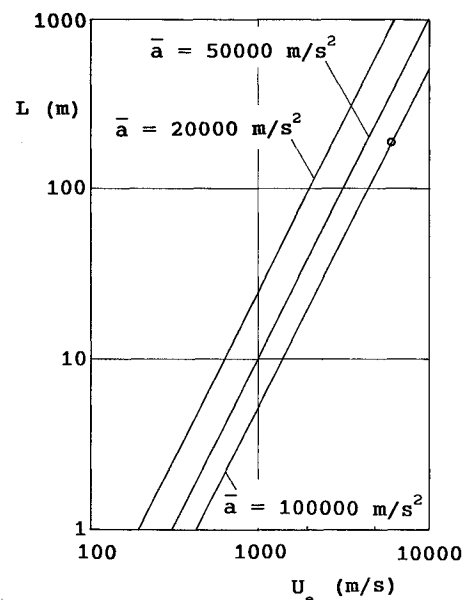


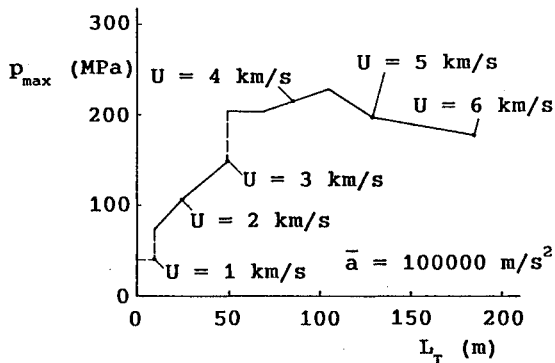
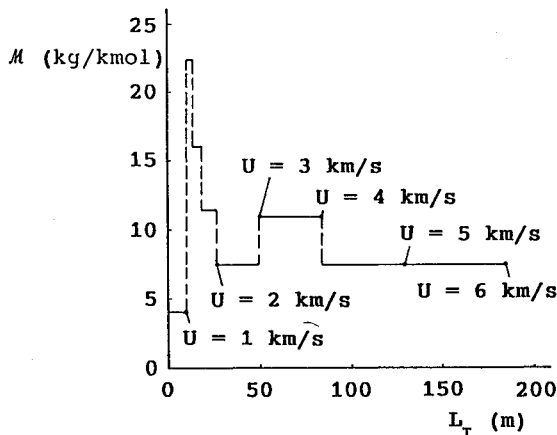
Fig. 3 Length of ram-tube as a function of terminal projectile velocity at different acceleration levels.

Table 2 Permitted acceleration levels for individual model components

Component	a , m/s ²
Model structure	$5 \times 10^5 - 10^6$
Piezotransducers at launch	10^5
Piezotransducers at recovery	2.5×10^5
Data transmission and electronics	7×10^5

Table 3 Composition of gas mixtures and pressure performance for $D_{\text{Proj}}/D_{T,\text{in}} = 0.77$.
Upper block: subdetonative mode, lower block: superdetonative mode

U , m/s	Mixture	p_{max}/p_1	p_{eff}/p_1	L_T , m
1125	$2\text{H}_2 + \text{O}_2 + 3.5\text{N}_2 + 0.5\text{CO}_2$	16.2	9.9	2.8
1425	$2\text{H}_2 + \text{O}_2 + 2.5\text{N}_2 + 1.5\text{He}$	19.1	10.9	5.0
1800	$2\text{H}_2 + \text{O}_2 + 1.15\text{N}_2 + 2.85\text{He}$	20.3	12.0	8.2
2300	$2\text{H}_2 + \text{O}_2 + 4\text{He}$	22.3	13.0	24.0
2600	$2\text{H}_2 + \text{O}_2 + 4\text{He}$	25.4	12.1	
3000	$2\text{H}_2 + \text{O}_2 + 4\text{He}$	29.6	10.1	
3600	$2\text{H}_2 + \text{O}_2 + \text{N}_2 + 3\text{He}$	40.5	13.6	35.0
4500	$2\text{H}_2 + \text{O}_2 + 4\text{He}$	45.8	14.7	100.0
5000	$2\text{H}_2 + \text{O}_2 + 4\text{He}$	39.4	14.1	
6000	$2\text{H}_2 + \text{O}_2 + 4\text{He}$	35.4	13.3	


Fig. 4 Maximum predicted pressures in the ram-tube for a fill pressure of 5 MPa.

Fig. 5 Distribution of propellant molecular mass along the length of the ram-tube.

some extent, and it will be one of the tasks of research to find out what this is. If the constraints turn out to be severe, special measures will have to be developed. It is possible that the same holds true for the region of impingement of the reflected shock on the shoulder of the sabot. Compared with the aerothermal problems, the structural strength against the external pressure is no problem, but just a matter of sufficient material thickness. To the best of present knowledge, the projectiles penetrate the diaphragms without suffering damage, or demanding special measures.^{9,13}

Model span and tube diameter $D_{T,\text{in}}$ roughly correspond, because the model's wings can be accommodated inside the projectile fins. Because the optimum effective projectile diameter $D_{\text{Proj,eff}}$ is, depending on velocity, $0.7 \times D_{T,\text{in}}$ to $0.85 \times D_{T,\text{in}}$, $m_{\text{Proj}}/A_{\text{cs,Proj}}$ attains a maximum value of 400 kg/m^2 for $m_{\text{Proj}} = 5 \text{ kg}$ and $D_{T,\text{in}} = 20 \text{ cm}$, and also for $m_{\text{Proj}} = 30 \text{ kg}$ and $D_{T,\text{in}} = 50 \text{ cm}$. Accordingly, for $a_{\text{Proj}} = 10^5 \text{ m/s}^2$ we

Table 4 Mass of gas needed for one shot at $T_i = 295 \text{ K}$

Component	m_{Prop} ($D_{T,\text{in}} = 20 \text{ cm}$)	m_{Prop} ($D_{T,\text{in}} = 50 \text{ cm}$)
Accelerator tube	98.60 kg	616.25 kg
Preaccelerator	1.28 kg	8.00 kg
Entire facility	99.88 kg	624.25 kg

Table 5 Consumption of gas species per shot for $D_{T,\text{in}} = 20 \text{ cm}$

Species	Standard volume per shot, m^3
H_2	78.54
O_2	39.27
N_2	14.98
He	142.91
or H_2	131.92
and N_2	10.99
CO_2	0.31
He (preaccelerator)	7.85

obtain $p_1 = 5 \text{ MPa}$. At $U_{\text{Proj}} = 3000 \text{ m/s}$ we assume transition from subdetonative to superdetonative combustion. Figure 4 shows a plot of peak pressure along the length of the tube for $p_1 = 5 \text{ MPa}$. The maximum value is 230 MPa, which requires a ratio of tube o.d. to i.d., $D_{T,\text{ex}}/D_{T,\text{in}} = 1.44$, for an assumed tube material tensile strength of $\sigma_{p,T} = 800 \text{ MPa}$, and $D_{T,\text{ex}}/D_{T,\text{in}} = 2.86$ for $\sigma_{p,T} = 600 \text{ MPa}$ for homogenous tubes.

The projectile velocity and propulsion mode determine the required molecular mass M of the gas mixture. Figure 5 shows the variation of M along the length of the tube. This variation in M was selected for optimum performance. The gradients of M require segmentation of the tube by thin diaphragms, a technique that has been demonstrated experimentally.¹¹ Table 3 gives the species ratios using H_2 and O_2 as propellants, and N_2 and He as inert components. Hydrogen can also be used as a diluent. For the first section of the accelerator tube we also need some CO_2 , and for the preaccelerator we use He. Table 4 shows the total gas consumption of two facilities, one with $D_{T,\text{in}} = 20 \text{ cm}$ and the other with $D_{T,\text{in}} = 50 \text{ cm}$, respectively, and Table 5 shows the species distribution.

Instead of He, a cheaper mixture of H_2 and N_2 or H_2 alone could be used as diluents. This change would reduce aerodynamic heating of the projectile: the real gas stagnation temperature decreases from ≈ 3600 to $\approx 2900 \text{ K}$ at 4200 m/s , and from ≈ 5300 to $\approx 3600 \text{ K}$ at 6000 m/s . All other conditions (masses, pressure, efficiency, etc.) remain unchanged. A disadvantage of H_2 as a diluent is that the excess H_2 may burn when the partially burnt propellants exit from the accelerator tube into the atmosphere, thus possibly necessitating some protective measures.

Model Sabot and Diaphragms

If the model is nestled in a sabot, it must be set free after acceleration. This is more complicated than, e.g., discarding the sabot of subcaliber antitank kinetic energy ammunition because the test models have a much smaller ratio of $m_{proj}/A_{cs,proj}$ than these very massive and heavy slender bodies made of tungsten or depleted uranium. Accordingly, the test models are much more susceptible to aerodynamic disturbances. As another consequence of limited difference in density and C_D between the model and sabot, the time of parallel flight and detrimental shock wave interaction between model and sabot pieces is longer. Moreover, the model is entirely surrounded by the sabot (e.g., Fig. 6). If separation is effected by aerodynamic force, the model will be exposed to strong shock waves over its entire length, as can be seen in Fig. 7, and disturbances affecting the nose region of the model will be particularly adverse.

It is therefore advisable to separate the model and sabot in a vacuum.¹⁴ A perforated tube section between the ram accelerator tube and the separation tank can be used to allow some of the acceleration gas to exit into the atmosphere (Fig. 8). In the ram accelerator the bulk of the gas moves rearward and exits at the vented coupling between the preaccelerator and ram accelerator. The entrance port to the separation tank is closed with a suitable diaphragm, which can easily be penetrated by the projectile.

Sabot separation in the vacuum tank can be achieved by external guidance of the sabot parts, as sketched in Fig. 8. The fins of the sabot are engaged in guide rails, which are bent outwards at the place of separation. This automatically separates the sabot parts from the model and ejects them into suitable catch chambers. The curvature of the guide rails, and accordingly, the length of the separation tank, depend on the permitted lateral acceleration $a_{n,s}$, and this in turn depends on the ratio of tensile strength of the fins $\sigma_{p,f}$ to the mass m_s of the corresponding sabot part. The lightest possible construction should be the goal, coinciding with the general intention to minimize the overall mass of the ram projectile,

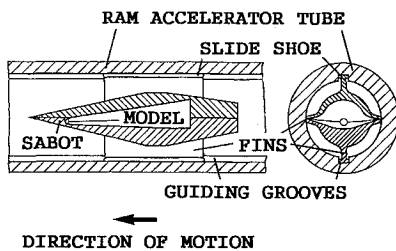


Fig. 6 Schematic of model nestled inside sabot having necessary ram projectile shape.

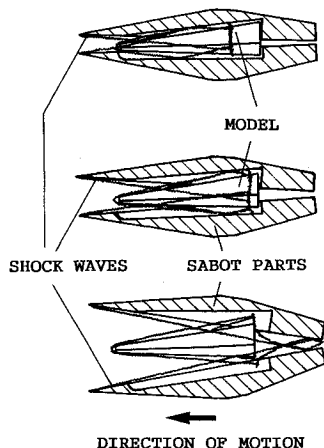


Fig. 7 Qualitative sketch of shock impingement between sabot parts and model.

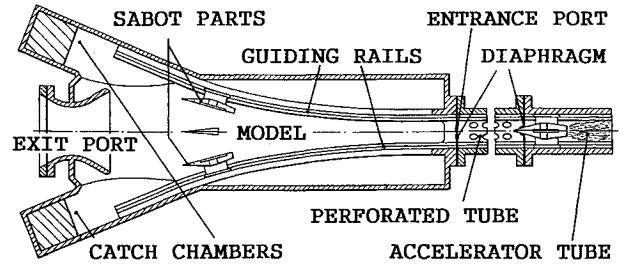


Fig. 8 Sketch of the sabot separation vacuum tank.

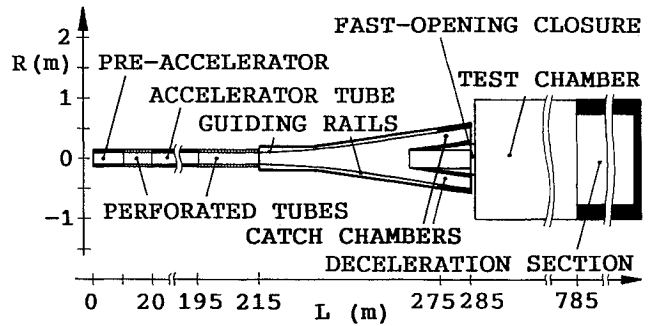


Fig. 9 Schematic of a ram-acceleration driven test facility for free-flying models.

and hence, the propellant needed for acceleration. With modern ceramic and fiber-reinforced materials this challenge should be met, because they have a significantly lower specific mass than conventional heat-resistant metals or alloys. Consider an example: if $a_{n,s}$ is 5000 m/s^2 , and the lateral distance to be covered is equal to $D_T/2 = 0.1$ and 0.25 m , respectively, for the 20- and 50-cm accelerator bores, we need $t = (D_T/a_{n,s})^{1/2}$, i.e., a time of 6.3 or 10.0 ms, respectively, for the two sizes of models. At 6000 m/s the required separation lengths are 38 and 60 m, respectively. Some extra length should be assigned for smoother curvature of the guide rails at the beginning of separation to minimize jerk load, and for attachment of the catch chambers.

The exit port of the separation tank needs an additional fast-opening closure to isolate the sabot separation vacuum tank from the gas-filled test section. The exit port should be opened just before the free-flying model arrives. When the closure opens, the gas from the test section will start to flow into the evacuated tank, towards the model. Suitable design of the closure will minimize the disturbance of the model by the inflow. This is also the case if the model passes into the free atmosphere instead of a confined test section.

Shallow guide grooves in the accelerator tube (see Fig. 6) fix the azimuthal position of the projectile during acceleration and ensure that the slide shoes encounter the guide rails of the separation tank.

The diaphragms that separate the different stages of the accelerator tube have only to withstand limited pressure differences, which occur inevitably during the filling process. The two diaphragms at the ends of the accelerator tube are more massive, because they must withstand a pressure differential of 5 MPa. As a consequence of very lightweight sabot design it may be necessary that these diaphragms (or, alternatively, fast-acting valves) have to be opened just before the projectile arrives.

Example: Design of Ram Accelerator

Figure 9 shows a schematic of a test facility with $D_T = 20 \text{ cm}$ to be used for task 1 in the Measuring Tasks section. Perforated tubes are installed at both ends of the ram accelerator tube for gas venting, most simply into the atmosphere. Their respective lengths are 10 m between the preaccelerator

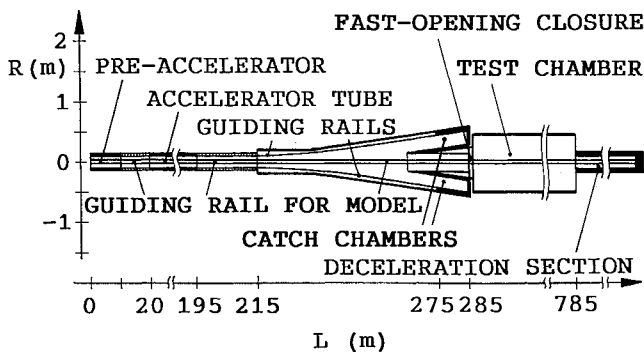


Fig. 10 Schematic of a ram-acceleration driven test facility for rail-guided models.

and the ram accelerator tube, and 20 m between the latter and the separation tank. The second perforated tube may also be replaced by just the guide rails. Protection of the surroundings should pose no serious problem.

The sabot separation vacuum tank shown has a total length of 70 m, of which 20 m are allotted to the sabot catch chambers. The beginning of the test section has to be placed after the end of the sabot catch chambers, because of their immediate vicinity to the model flight path. A tube surrounds the model flight path towards the fast-opening closure, which opens to let the model pass by. If the test gas is not air, this closure is preferably a valve, which closes immediately after the model passes by to minimize the loss of test gas. Otherwise, a diaphragm whose rupturing is externally controlled can be used as well.

The test chamber length L_{TC} in Fig. 9 is 500 m, providing about 83 ms of testing time for a model velocity of 6000 m/s. The test chamber diameter $D_{TC} = 2$ m does not allow for more than minimal erratic lateral motion. If the test section volume V_{TC} has to be minimized, the model can be guided, e.g., by a rail, as is shown in Fig. 10. In any case, L_{TC} should be adaptable to the effective test time needed.

Models with a speed of 6000 m/s are likely to cause considerable damage to test chamber structures in case of an accidental hit. Moreover, the destroyed model will produce small particles and gases of decomposition that will contaminate the test chamber, and larger fragments that may damage the instrumentation. As a consequence, in some cases it could be advantageous to use an inflatable, balloon-like test section instead of a massive, rigid one. A misguided model would then simply penetrate the wall without suffering total destruction, the hole could be patched, and in a favorable case the damage would be limited to just the loss of the test gas. The flexible test chamber could readily be varied in length, or folded if tests are to be carried out in ambient air, e.g., as noted in task 2 in the Measuring Task section.

Recovery of models moving at a velocity of 6 km/s is a very difficult operation and necessitates in every case a deceleration section of considerable length, and cross section, if some lateral motion of the models is permitted.¹⁴ If the model is also guided during flight in the test section, it can be decelerated in a tube filled with gas¹⁶ that gets compressed by the model.

If the facility is used for task 2, the models preferably fly through an unconfined atmospheric test range, where instruments for external measurements may be disposed as desired. In this case construction of a deceleration section is not feasible, because (accidental) deviation from the predicted flight path may be 100 m or more, depending on actually attained model shape and attitude. Hence, deceleration in the unconfined atmosphere is the best choice. The area necessary for safety may be available near the seashore. Moreover, recovery is easier at sea, if the remnant of the model is buoyant and emits signals. During the long flight, wings, fins, and nose

tips of the model will ablate and should be designed as expendable parts, which protect the valuable interior instrumentation. Of course, deceleration by the atmosphere can also be used for task 1 experiments.

Conclusions

For hypervelocity aerodynamic testing, accelerated models and a quiescent test atmosphere give greater freedom in choice of test gas state and composition. Test times greater than 10 ms can be easily achieved only by using accelerated models. This is mainly due to the aerothermal load on test facilities such as shock tunnels and Stalker tubes, particularly their nozzle throats, which can absorb only a limited amount of energy from the high enthalpy gas flow.

Similar aerothermal loads, to which the sabot is subjected during the acceleration, pose a technical challenge to the ram accelerator projectile as well. Nevertheless, ablation or erosion do not affect the test flow quality, but just the stability of the sabot. In view of novel materials such as carbon fiber reinforced carbon, or advanced ceramics, these problems should be solvable by careful selection of the sabot materials and tailoring of their composition to the heat flux history.

The state of transducer technology, telemetry, data storage techniques, and data processing makes it possible to use free-flying models with on-board instrumentation, to carry out measurements that traditionally could be performed only in test-flow accelerating facilities. For acceleration of these models, a ram accelerator facility is very suitable. In contrast to gas guns a ram accelerator can bring models to hypervelocity with arbitrary acceleration, thus allowing for delicate on-board installations. The propellant expense for acceleration of models to 6000 m/s is just about 20 times the model mass. Moreover, in view of its capability, the ram accelerator test facility is comparatively compact, and because just the essential mass, i.e., the model, is accelerated, it is also favorable with respect to safety considerations.

References

- Smeets, G., and Naumann, K. W., "Generation of Test Flows for Aeroballistic Experiments with the ISL Shock Tubes," French-German Research Inst., Rept. 113/86, (in German and French), Saint-Louis, France, 1989.
- Hornung, H., Sturtevant, B., Belanger, J., and Sanderson, S., "Performance Data of the New Free Piston Shock Tunnel T5 at GALCIT," *Shock Waves*, edited by K. Takayama, Vol. II, *Proceedings of the 18th International Symposium on Shock Waves* (Sendai, Japan), Springer-Verlag, Berlin, 1991, pp. 603-610.
- Naumann, K. W., Ende, H., Mathieu, G., and George, A., "Millisecond Aerodynamic Force Measurement with Side-Jet Model in the ISL Shock Tunnel," *AIAA Journal*, Vol. 31, No. 6, 1993, pp. 1068-1074.
- Neumann, R. D., "Requirements in the 1990's for High Enthalpy, Ground Test Facilities for CFD Validation," *AIAA Paper 90-1401*, June 1990.
- Seigel, A. E., "The Theory of High Speed Guns," *AGARDograph 91*, NATO, Advisory Group for Aerospace Research and Development, Paris, France, 1965, pp. 21, 22.
- Berggren, R. E., and Reynolds, R. R., "The Light Gas Gun Model Launcher," *Ballistic-Range Technology*, edited by T. N. Canning, A. Seiff, and C. S. James, *AGARDograph 138*, NATO, Paris, 1979, Ch. 2.
- Beck, W. H., Eitelberg, G., McIntyre, T. J., Baird, J. P., Lacey, J., and Simon, H., "The High Enthalpy Shock Tunnel (HEG) in Göttingen," *Shock Waves*, edited by K. Takayama, Vol. II, *Proceedings of the 18th International Symposium on Shock Waves* (Sendai, Japan), Springer-Verlag, Berlin, 1991, pp. 677-682.
- Morrison, W. R. B., Stalker, R. J., and Duffin, J., "New Generation of Free-Piston Shock Tunnels," *17th International Symposium on Shock Tubes and Waves, AIP Conference Proceedings 208*, American Inst. of Physics, New York, 1990, pp. 582-587.
- Bruckner, A. P., Knowlen, C., and Hertzberg, A., "Application of the Ram Accelerator for Hypervelocity Aerothermodynamic Testing," *AIAA Paper 92-3949*, July 1992.
- Rateau, P. H., and Kocher, L., "Quartz-Controlled Miniaturized

Telemetry Transmitter for High Acceleration Loads up to over 50000 g," French-German Research Inst., TR 506/89 (in French), Saint-Louis, France, 1989.

¹¹Hertzberg, A., Bruckner, A. P., and Knowlen, C., "Experimental Investigation of Ram Accelerator Propulsion Modes," *Shock Waves*, Vol. 1, No. 1, 1991, pp. 17-25.

¹²Giraud, M., Legendre, J.-F., and Simon, G., "Ram Accelerator Studies in 90 mm Caliber," French-German Research Inst., CO 233/92, Saint-Louis, France, 1992.

¹³Kruczynski, D., "New Experiments in a 120-mm Ram Accelerator at High Pressures," AIAA Paper 93-2589, June 1993.

¹⁴Naumann, K. W., and Smeets, G., "Ram-Accelerator as a Hypervelocity Testing Facility," French-German Research Inst. (in German), N 602/90, Saint-Louis, France, 1990.

¹⁵Phillips, D. C., "Fibre Reinforced Ceramics," *Handbook of Composites*, edited by A. Kelly and S. T. Mielko, Vol. 4, Elsevier, Amsterdam, 1983.

¹⁶Hertzberg, A., Bruckner, A. P., and Knowlen, C., "The Ram-Accelerator as a Hypersonic Test Facility," AIAA 16th Aerodynamic Ground Testing Conf., Univ. of Washington, Aerospace and Energetics Research Program, Dept. of Aeronautics and Astronautics, FL 10, Seattle, WA, June 1990 (Post-deadline paper).

Recommended Reading from the AIAA Education Series

Composite Materials for Aircraft Structures

Brian C. Hoskin and Alan A. Baker, editors

An introduction to virtually all aspects of the technology of composite materials as used in aeronautical design and structure. Discusses important differences in the technology of composites from that of metals: intrinsic substantive differences and their implications for manufacturing processes, structural design procedures, and in-service performance of the materials, particularly regarding the cause and nature of damage that may be sustained.

1986, 237 pp, illus, Hardback
ISBN 0-930403-11-8
AIAA Members \$43.95
Nonmembers \$54.95
Order #: 11-8 (830)

Place your order today! Call 1-800/682-AIAA



American Institute of Aeronautics and Astronautics

Publications Customer Service, 9 Jay Gould Ct., P.O. Box 753, Waldorf, MD 20604
FAX 301/843-0159 Phone 1-800/682-2422 8 a.m. - 5 p.m. Eastern

Sales Tax: CA residents, 8.25%; DC, 6%. For shipping and handling add \$4.75 for 1-4 books (call for rates for higher quantities). Orders under \$100.00 must be prepaid. Foreign orders must be prepaid and include a \$20.00 postal surcharge. Please allow 4 weeks for delivery. Prices are subject to change without notice. Returns will be accepted within 30 days. Non-U.S. residents are responsible for payment of any taxes required by their government.